Transformation of Inclusions in Solid GCr15 Bearing Steels During Heat Treatment

Gong Cheng, Weifu Li, Xianguang Zhang and Lifeng Zhang *

School of Metallurgical and Ecological Engineering, University of Science and Technology Beijing (USTB), Beijing 100083, China; chenggong_ustb@163.com (G.C.); 13333109538@163.com (W.L.); xgzhang@ustb.edu.cn (X.Z.)

* Correspondence: zhanglifeng@ustb.edu.cn; Tel.: +86-010-6233-2267

check for updates

Abstract: Laboratory heating experiments with a varied holding time of GCr15 bearing steels at 1498 K were performed to study the transformation of inclusions in solid GCr15 bearing steels during high temperature diffusion processes. Heating experiments at 1573 and 1648 K were also carried out to study the effect of these heating temperatures. Experimental results showed that inclusions transformed from Al_2O_3-CaO-(MgO) to Al_2O_3-CaS-(MgO-CaO) when the heat treatment was in the range of 1498 to 1648 K due to reactions between Al and S in the steel matrix and CaO in the inclusions. This is in good agreement with thermodynamic calculations. Moreover, the size of the inclusions hardly changed after heat treatment. The transformation rate of the inclusions depended strongly on both the heating temperature and the size of the inclusions. Kinetic analyses on the transformation of inclusions during heat treatment were performed based on a simplified analytical model. The mass transfer coefficients of CaO and CaS in inclusions were calculated, which ranged from 0.73×10^{-10} to 4.48×10^{-10} m/s.

Keywords: heat treatment; transformation; mass transfer coefficient

1. Introduction

Bearing steels are widely applied in machinery manufacturing, railway transportation, automobile manufacturing, national defense industries, and other fields [1]. It is well known that the mass fraction, composition, size, morphology, and distribution of non-metallic inclusions have an important influence on the rolling contact fatigue (RCF) life of bearing steels [2–5]. The demand for the RCF life of bearing steels becomes more stringent, which requires a better control of steel cleanliness. The RCF life of Al-killed bearing steels can be increased 30 times by decreasing the oxygen content from 30 ppm to 5 ppm [6]. Besides, the RCF life is also closely related to the composition of inclusions in bearing steels. It is found that titanium nitride inclusions are more harmful than oxide inclusions with the same size. The detrimental effect of a 7 μm TiN inclusion is equivalent to that of a 25 μm oxide inclusion. However, large globular calcium aluminate inclusions are the most detrimental to bearing steels [2].

Extensive research on the formation, removal, and modification of non-metallic inclusions in the molten steel at steelmaking temperatures have been conducted, such as the calcium treatment [7–15], the rare earth element treatment [16,17], slag refining [18–22], and reoxidation [23,24]. However, less attention has been paid to the variation of oxide inclusions in the solid steel during heat treatment. It was reported that MnO-SiO_2 oxide inclusions in Type 304 stainless steels may transform to MnO-Cr_2O_3 during heat treatment in the range of 1273 to 1623 K [25–27] The contents of Mn, Si, and Cr in the steel had a strong influence on the transformation [28,29]. It was found that Al-Ca-O-S complex inclusions were the predominating particles in EH36 shipbuilding steels, but the TiN ones were profusely populated after being heated at 1473 K [30,31]. CaO-Al_2O_3 type of inclusions in pipeline

steels transformed into Al$_2$O$_3$-CaS type after heat treatment in the range of 1273 to 1673 K [27,32]. Yang et al. also investigated the transformation of inclusions in pipeline steels during solidification and cooling [33]. For a high temperature diffusion process of high carbon chromium bearing steels to reduce the segregation of bloom and precipitation of ribbon type carbide as well as aliquation carbide, 1473 K is usually utilized [34]. However, the transformation of inclusions in Al-killed GCr15 bearing steels during high temperature diffusion processes has rarely been studied.

Thermodynamic models [35,36] and kinetic models [37–40] have been established to predict the compositions of steel, slag, and inclusions in the molten steel, as well as the precipitation of sulfides [41,42] and nitrides [43,44] during cooling and solidification. In the current work, the transformation of inclusions in a GCr15 bearing steel during high temperature diffusion processes was investigated through laboratory experiments, thermodynamic analyses and kinetic analyses. Isothermal heat treatment of the Al-killed GCr15 bearing steel was performed at varied temperatures that ranged from 1498 to 1648 K under an argon atmosphere.

2. Experimental Procedure

Industrial trails for the production of a GCr15 bearing steel by a route of "EAF-LF refining-vacuum degassing-bloom CC-hot rolling" were performed. The molten steel was casted into 320 mm × 480 mm blooms. Before hot rolling, the bloom was heated for 3 h, 7 h, or 12 h in the range of 1493 to 1503 K as a high temperature diffusion process. The chemical composition of the bearing steel used in this study is listed in Table 1.

Table 1. Chemical composition of the GCr15 bearing steel used in the current study (mass %).

C	Cr	Si	Mn	P	S	O	Mg	Ca	Als
1	1.563	0.3	0.39	0.0115	0.0031	0.0007	0.0003	0.0003	0.015

The cylindrical steel sample with a 34 mm diameter was taken from the tundish and quenched in water. The quenched steel sample was machined into sectors (each measuring approximately 17 mm × 10 mm with an angle of 60°), as shown in Figure 1. Next, the machined samples were heated under an argon atmosphere at 1498, 1573, or 1648 K for various periods from 5 min to 12 h, respectively, in a Si-Mo resistance furnace (SHIMADEN FP21, Tokyo, Japan), followed by water quenching. The schematic of experimental procedures is shown in Figure 2.
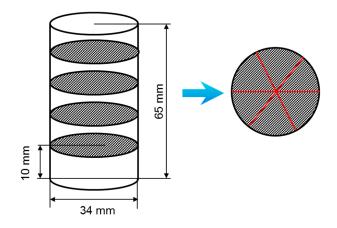

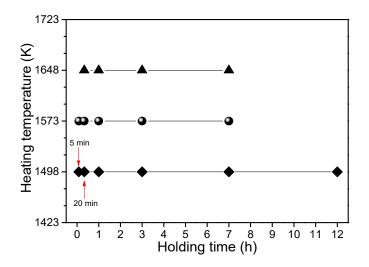**Figure 1.** Schematic of the machined samples.

Figure 2. Heating experiments of steel under three temperature conditions.

Quenched steel samples were mounted in epoxy resin, ground and polished. The size, composition, morphology and amount of inclusions in steel samples were analyzed by an automatic SEM-EDS equipment (FEI, Pittsburgh, PA, USA). The scanned area was over 60 mm^2 for each sample.

3. Change of Inclusion Composition During Heating Treatment

3.1. Effect of Holding Time on the Transformation of Inclusions in the Steel During Heating

The composition and size of the inclusions in the steel before and after the heat treatment at 1498 K with varied holding time are shown in Figure 3. As shown in Figure 3a, the inclusions were mainly MgO·Al$_2$O$_3$ and Al$_2$O$_3$-CaO-(MgO) which represents Al$_2$O$_3$-CaO with limited MgO content, before heat treatment. A typical inclusion with mapping and line scanning is shown in Figure 4. The average composition of inclusions was 15.42 wt % MgO-63.76 wt % Al$_2$O$_3$-17.18 wt % CaO-3.64 wt % CaS. According to Figure 3b, after being annealed at 1498 K for 5 min, the average content of CaO in the inclusions decreased while the CaS content slightly increased. After 20 min, the average content of CaO in the inclusions decreased from 17.18 to 9.36 wt % while the CaS content increased from 3.64 to 13.06 wt %, as shown in Figure 3c. Figure 5 shows a typical inclusion in the steel after being held at 1498 K for 1 h, which was the MgO-Al$_2$O$_3$ core enveloped by CaS. The average composition of inclusions in the steel had no obvious change when the holding time was longer than 3 h, according to Figure 3e–g. The average composition of the inclusions in the steel after being held at 1498 K for 12 h was 13.20 wt % MgO-69.94 wt % Al$_2$O$_3$-4.12 wt % CaO-12.73 wt % CaS. An irregular shaped MgO-Al$_2$O$_3$-CaS inclusion was observed after the steel was held at 1498 K for 12 h, as shown Figure 6, which was MgO-Al$_2$O$_3$ in the core and CaS in the periphery. Wang et al. investigated the effect of CaS on the evolution of CaO-Al$_2$O$_3$ inclusions in low-carbon Al-killed and Ca-treated steels during the solidification process [7]. It was found that the inclusions were originally liquid and spherical, and transformed to an irregular state during solidification due to the reaction between CaO-Al$_2$O$_3$ inclusions with the dissolved sulfur and aluminum in the steel, resulting in the formation of dense CaS shells around the inclusions. The effect of the holding time on the average composition of inclusions at 1498 K is shown in Figure 7. It indicates that inclusions are transformed from Al$_2$O$_3$-CaO-(MgO) to Al$_2$O$_3$-CaS-(MgO-CaO). Error bars represented the 95% confidence interval of the mean composition.
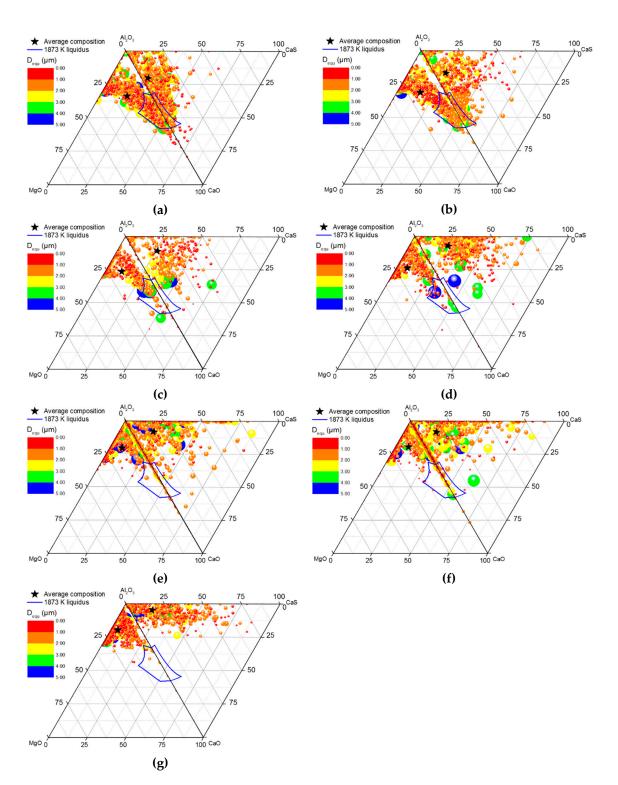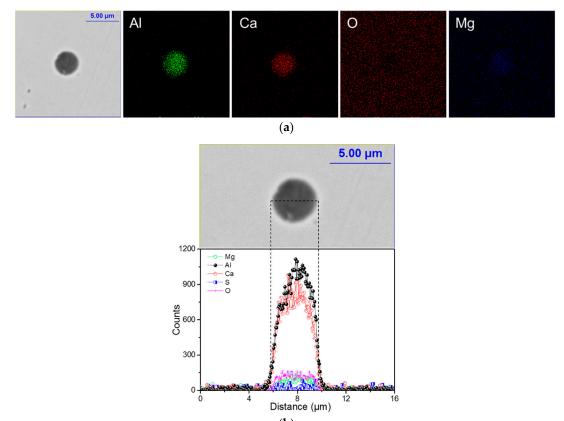
Figure 3. Composition and size of inclusions in steel samples: (**a**) Before and after heat treatment at 1498 K for (**b**) 5 min, (**c**) 20 min, (**d**) 1 h, (**e**) 3 h, (**f**) 7 h, (**g**) 12 h.

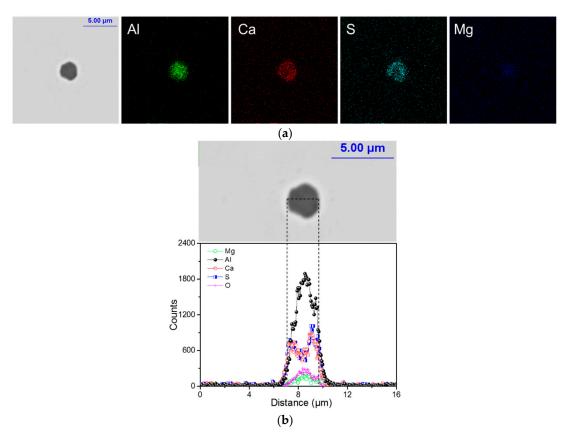**Figure 4.** Typical inclusion in the steel before heat treatment: (**a**) Mapping, (**b**) line scanning.

Figure 5. Typical inclusion in the steel after 1 h heat treatment at 1498 K: (**a**) Mapping, (**b**) line scanning.

(**a**)
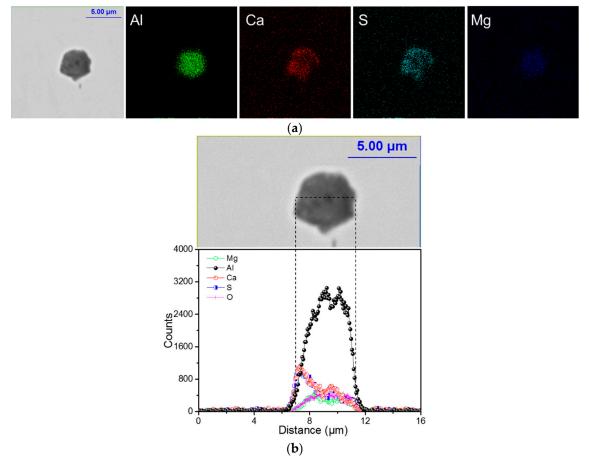

(**b**)

Figure 6. Typical inclusions in the steel after 12 h heat treatment at 1498 K: (**a**) Mapping, (**b**) line scanning.
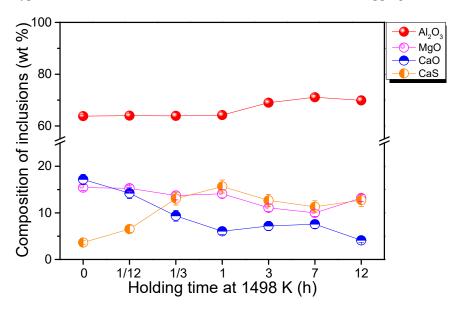

Figure 7. Effect of holding time on the average composition of inclusions at 1498 K.

The evolution of the average content of each component in the inclusions as a function of the inclusion diameter is shown in Figure 8. According to Figure 8a, before heat treatment, inclusions larger than 3 μm were mainly calcium aluminate. As for inclusions smaller than 3 μm, the CaO content increased with the increase of the diameter, and the contents of Al_2O_3 and MgO decreased.

As shown in Figure 8b, after being held at 1498 K for 1 h, the CaO content in inclusions with the size of 1–4 µm decreased while the CaS content increased. As for the inclusions less than 3 µm, the average composition of the inclusions is almost the same regardless of the size. The CaO content of the inclusions decreased to 6 wt % after the steel was heated for 3 h, as shown in Figure 8c. The composition of inclusions with different sizes varied slightly with a longer holding time, as shown in Figure 8d. All the above experimental results indicated that the composition of small inclusions varied more severely than large ones. According to Figure 8, the CaS and Al$_2$O$_3$ content of the inclusions increased, and the CaO content decreased with the increase of the holding time, especially for large inclusions. The main reaction that occurred in the steel during heat treatment at 1498 K is as follows:

$$3(CaO)+3[S]+2[Al] \rightarrow 3(CaS)+(Al_2O_3) \tag{1}$$

The variation in the number density and average diameter of the inclusions in the steel are shown in Figures 9 and 10, respectively. The number density of inclusions varied slightly with time when the steel was held at 1498 K. The average diameter of the inclusions in the steel decreased after heating, especially after 12 h heat treatment at 1498 K.
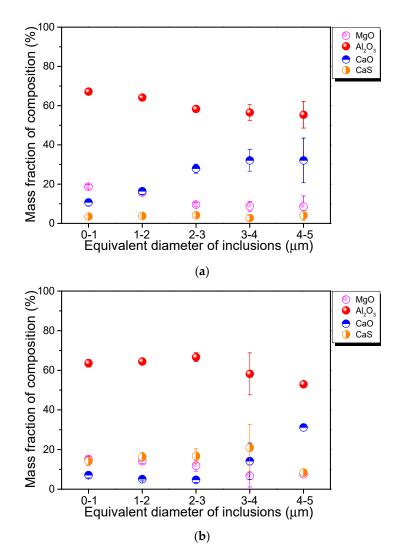

(**a**)

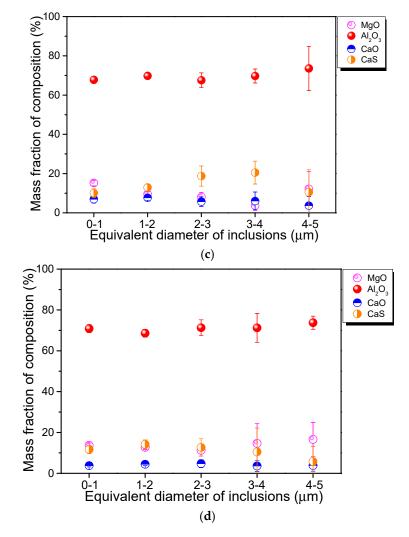(**b**)

Figure 8. *Cont.*

Figure 8. Evolution of the average mass fraction of each component in inclusions as a function of their diameter: (**a**) Before and after heat treatment at 1498 K for (**b**) 1 h, (**c**) 3 h, (**d**) 12 h.
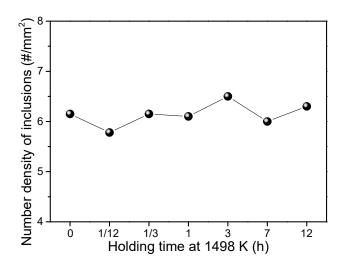

Figure 9. Variation in the number density of inclusions in the steel during heat treatment at 1498 K.

The variation in the size distribution of the inclusions in the steel against the holding time is shown in Figure 11. The number of small inclusions increased after heat treatment at 1498 K, especially

heat treatment of 7 and 12 h. Less variation in the area fraction of the inclusions in the steel with holding time was observed. The results are shown in Figure 12.
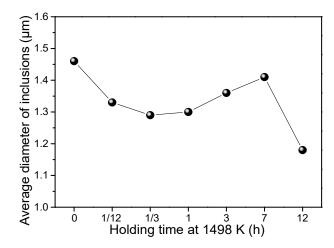

Figure 10. Variation in the average diameter of inclusions in the steel during heat treatment at 1498 K.
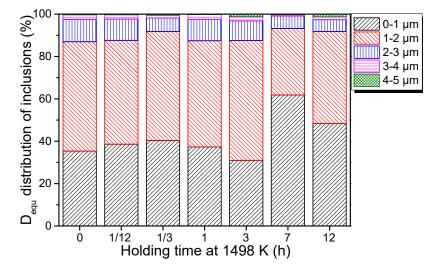

Figure 11. Variation in the size distribution of inclusions in the steel during heat treatment at 1498 K.
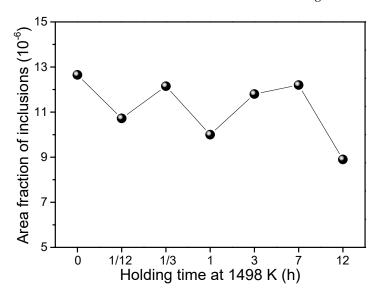

Figure 12. Variation in the area fraction of inclusions in the steel during heat treatment at 1498 K.

3.2. Effect of Temperature on the Transformation of Inclusions in the Steel During Heating

The effect of holding time on the average composition of the inclusions in the steel during heat treatment at 1573 K is shown in Figure 13. After heating for 5 min at 1573 K, the average content of CaS in inclusions increased while the CaO content slightly decreased. The average content of CaO in inclusions decreased from 17.18 wt % to 5.33 wt % and the CaS content increased from 3.64 wt % to 19.41 wt % after heating for 20 min at 1573 K. The average composition of inclusions slightly varied after heating for 1 h or longer at 1573 K. The average composition of inclusions in the steel after heating for 7 h at 1573 K was 17.10 wt % MgO-58.77 wt % Al_2O_3-2.60 wt % CaO-21.53 wt % CaS. The CaS content of inclusions increased and the CaO content decreased with time at 1573 K.
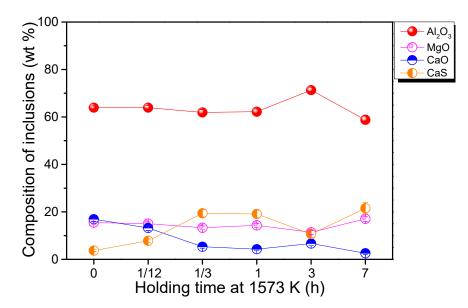

Figure 13. Effect of holding time of heating on the average composition of inclusions in the steel heated at 1573 K.

The effect of holding time on the average composition of inclusions in the steel heated at 1648 K is shown in Figure 14. After heating for 20 min at 1648 K, the content of CaS in inclusions increased from 3.64 wt % to 7.59 wt %, while the CaO content decreased from 17.18 wt % to 11.95 wt %. The content of CaO in inclusions slightly decreased and that of CaS further increased after the steel was heated for 1 h at 1648 K. After heating for 3 h at 1648 K, the CaO content decreased to 7.28 wt % and the CaS content increased to 18.13 wt %. The average composition of inclusions varied little after the steel was heated for 7 h. The CaS content in the inclusions increased and the CaO content decreased with time at 1648 K.

Figure 15 shows the composition of inclusions against the annealing temperature at a fixed holding time of 7 h. With the increase of temperature, the CaS content in inclusions increased, while the CaO content decreased significantly, and the Al_2O_3 and MgO contents slightly varied. According to the above results, the main reaction that occurred in the steel during heat treatment at 1573 and 1648 K is:
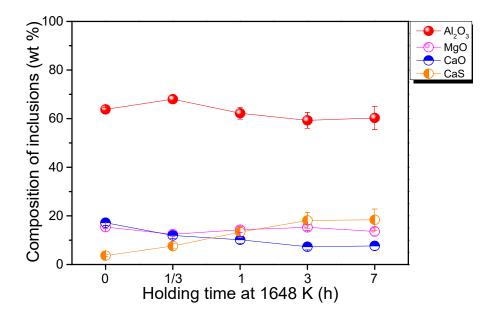
$$(CaO) + [S] = (CaS) + [O] \tag{2}$$

Figure 14. Effect of holding time on the average composition of inclusions in the steel during annealing at 1648 K.

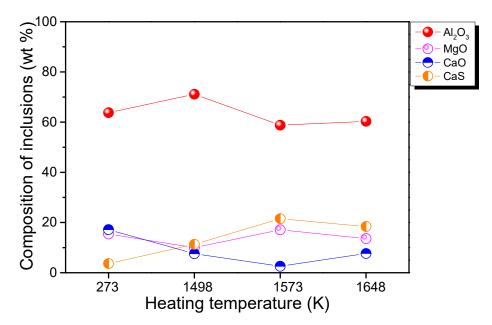**Figure 15.** Effect of temperature on the average composition of inclusions in the steel with same holding time (7 h).

Figure 16 shows the effect of the holding time and temperature on the size of the inclusions in the steel. The average size of inclusions decreased slightly with the increase of temperature and holding time, implying that small inclusions were generated, especially CaS inclusions.
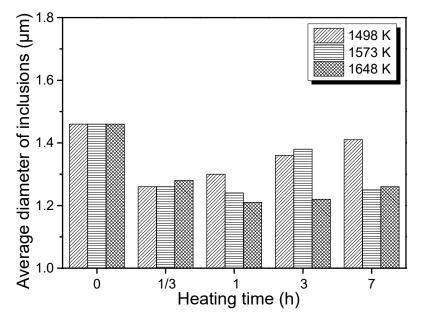
Figure 16. Effect of holding time and temperature on the size of inclusions in the steel during heat treatment.

4. Thermodynamic Considerations on the Transformation of Inclusions in the Steel During Heat Treatment

The comprehensive transformation of inclusions in the bearing steel consisted of three parts: Self-precipitation of inclusions, new precipitates from the steel, and the transformation of the inclusions from the reaction between steel and inclusions. In order to understand the transformation of the inclusions in the steel during heat treatment, thermodynamic calculations were carried out.

4.1. Self-Precipitation of Inclusions with the Decrease of Temperature only Considering Inclusions

The precipitation of phases in the inclusions with the decrease of temperature only considering the inclusions was calculated using FactSage 7.0 (Thermfact/CRCT & GTT-Technologies, Aachen, Germany) with the Ftoxid database. The result is shown in Figure 17. The initial composition of inclusions was 15.42 wt % MgO-63.76 wt % Al_2O_3-17.18 wt % CaO-3.64 wt % CaS, which was the average composition of inclusions in the bearing steel before heat treatment. According to Figure 17, at 1773 K, the liquid and solid phase of $MgO \cdot Al_2O_3$ exist in inclusions. As the temperature decreases, solid $CaO \cdot Al_2O_3$ precipitates accompanied with the decrease in the liquid phase, and the $MgO \cdot Al_2O_3$ ones slightly increase. The liquid phase disappears at 1611 K, along with the precipitation of solid $3CaO \cdot 2MgO \cdot Al_2O_3$. The calculated results show that the precipitation of phases in the inclusions at heat treatment temperature did not result from the formation of CaS inclusions, and the CaO content in the inclusions hardly decreased, indicating that the variation of the composition of inclusions in the bearing steel was not caused by self-precipitation of inclusions during heat treatment.
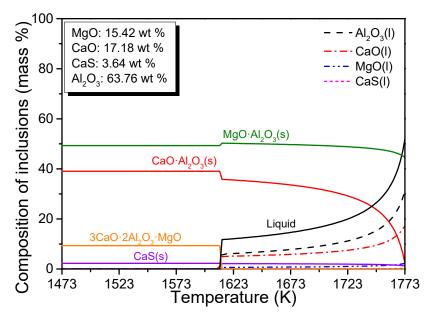
Figure 17. Precipitation of phases in inclusions with the decrease of temperature only considering inclusions.

4.2. Precipitation of Inclusions in the Bearing Steel at Various Temperature with Consideration of Steel

For the steel with 7 ppm T.O. (total oxygen content), which was used in the current experiments, the precipitation of inclusions in the bearing steel at various temperatures with consideration of steel was calculated using FactSage 7.0 with the FactPS, FToxid, and Fsstel databases. The result is shown in Figure 18. Due to the similarity of transformations under different conditions according to Figure 18, only the comprehensive transformation of inclusions in the bearing steel is illustrated in detail. As shown in Figure 18a, at the initial decreasing of temperature, inclusions in the bearing steel are liquid oxides and solid $MgO \cdot Al_2O_3$ ones. As the temperature decreases, the amount of spinel phase increases and a small amount of solid MgO inclusions forms. At 1737 K, solid CaS inclusions start to precipitate and the content of solid $MgO \cdot Al_2O_3$ further increases with the decrease of liquid phase. The liquid phase disappears at 1719 K. Trace amount of solid MgO and MgS precipitates in bearing steels with the further decrease of temperature.

During heat treatment in the temperature range of 1498 to 1648 K, the main equilibrium inclusion phases are solid CaS and $MgO \cdot Al_2O_3$. By combining the content of each phase, the average composition of inclusions during heat treatment can be obtained, as shown in Figure 19. The CaO content of inclusions decreases to zero when the temperature decreases to 1719 K, and the CaS content in inclusions increases significantly. Moreover, the Al_2O_3 and MgO contents of inclusions vary slightly, indicating that the transformation from CaO into CaS in inclusions mainly occurs during heat treatment.
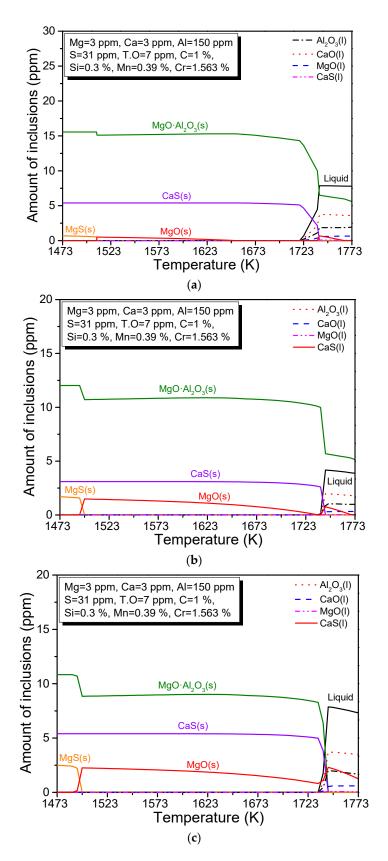
Figure 18. Precipitation of inclusions in the bearing steel at various temperature with 7 ppm T.O.: (**a**) Comprehensive transformation, (**b**) new precipitates from the steel, (**c**) transformation of inclusions from the reaction between steel and inclusions.
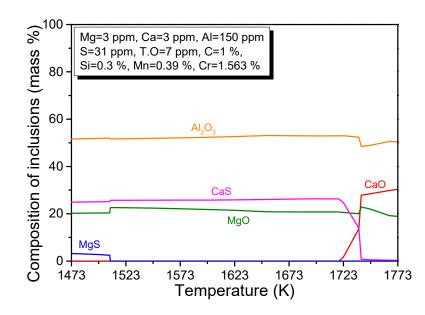
Figure 19. Evolution of the composition of inclusions in bearing steels at various temperature considering the steel with 7 ppm T.O.

The comprehensive transformation of inclusions in the bearing steel at various temperatures considering the steel with 10 ppm T.O is quite different. Liquid oxides and solid $MgO·Al_2O_3$ form between 1717 K and 1773 K during the solidification of the steel when T.O content is 10 ppm, as shown in Figure 20. The amount of $MgO·Al_2O_3$ inclusions increases with the decrease of temperature. Solid CaS inclusions begin to precipitate at 1717 K. Solid $CaO·Al_2O_3$ inclusions generate and liquid phase disappears at 1698 K. As the temperature further decreases, solid $CaO·2Al_2O_3$ and $CaO·2MgO·8Al_2O_3$ precipitate successively, along with the disappearance of $CaO·Al_2O_3$ and $CaO·2Al_2O_3$ in succession. According to the calculated results above, it can be concluded that the steel composition has an important influence on the transformation of inclusions in the bearing steel during heat treatment.
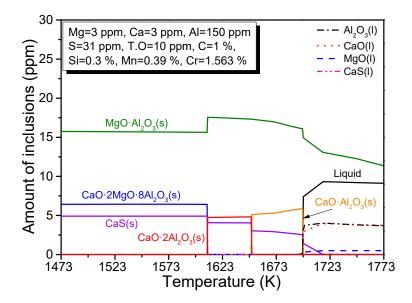

Figure 20. The comprehensive transformation of inclusions in bearing steels at various temperature considering the steel with 10 ppm T.O.

Figure 21 shows the comparison of the experimental results and thermodynamic calculation results with the decrease of temperature. In the temperature range of 1498 to 1648 K, according to

the comprehensive calculation result, the composition of the inclusions hardly varies and consists of 20.95 wt % MgO-53.03 wt % Al_2O_3 -26.02 wt % CaS. The average composition of inclusions measured in the bearing steel after heat treatment at different temperature was almost the same and comprised of 17.10 wt % MgO-58.77 wt % Al_2O_3-2.60 wt % CaO-21.53 wt % CaS after heat treatment at 1573 K. The calculated and measured results are in good agreement with each other and show that the transformation of inclusions happens during heat treatment. However, minor deviations between experimental and calculated values were also observed. Thermodynamic calculation results were obtained based on the equilibrium state, which means a sufficient reaction time and no consideration of the reaction between the slag and refractories. However, in heat treatment experiments in the current work, the reaction time is insufficient to reach the equilibrium, resulting in the minor deviation between the experimental and calculated results.
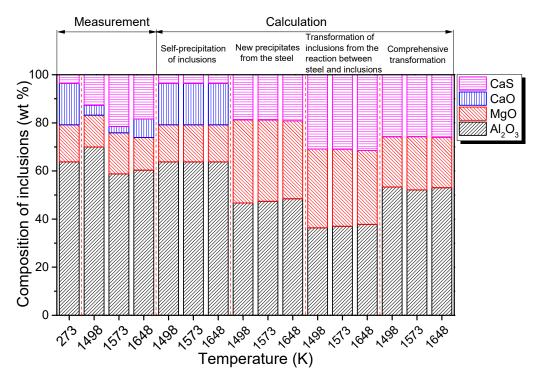

Figure 21. Comparison of experimental results and thermodynamic calculation results with the decrease of temperature.

5. Kinetic Analyses on the Transformation of Inclusions During Heat Treatment

As shown in Figure 22, the initial inclusions in the steel were mainly Al_2O_3-CaO-(MgO) and $MgO \cdot Al_2O_3$ before heat treatment. During heat treatment, the high temperature accelerated the diffusion of elements in the steel matrix such as [Al] and [S]. Reactions between [Al] and [S] in the steel matrix and [Ca] and [O] in Al_2O_3-CaO-(MgO) inclusions were promoted, which were expressed by Equations (3)–(5). Besides, $MgO \cdot Al_2O_3$ phases were formed by the reaction between Al_2O_3 and MgO inside inclusions, as shown in Equation (6). The initial $MgO \cdot Al_2O_3$ inclusions in the steel before heat treatment did not transform during heat treatment. After the steel was heated at a high temperature for a long time, the inclusions in the steel were mainly $MgO \cdot Al_2O_3$ and $MgO \cdot Al_2O_3$ enveloped by CaS. It should be pointed out that Equations (3)–(6) appeared to dominate during heat treatment at 1498 K, resulting in the increase of Al_2O_3 and CaS, as well as the decrease of CaO. However, Equations (3), (4), and (6) seemed to dominate during heat treatment at 1573 and 1648 K, only leading to the increase of CaS and the decrease of CaO.

$$(CaO) = [Ca] + [O] \tag{3}$$

$$[Ca] + [S] = (CaS) \tag{4}$$

$$2[Al] + 3[O] = (Al_2O_3) \tag{5}$$

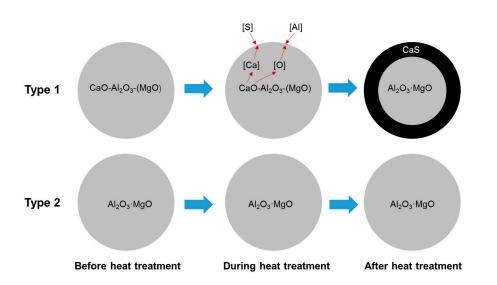$$x(MgO) + y(Al_2O_3) = xMgO \cdot yAl_2O_3 \tag{6}$$

Figure 22. Schematic of the transformation mechanism of inclusions in the bearing during heat treatment.

According to thermodynamic calculation results in Section 4, the CaS content, as well as the CaO content, in the inclusions at the equilibrium state was a little distinct at different temperatures. Thus, the transformation of the inclusions could be treated as the same from the thermodynamic perspective. However, under the experimental conditions, according to Figure 7, Figure 13, and Figure 14, the evolution of the composition of inclusions as a function of holding time at different temperatures was diverse, which should be attributed to the transformation kinetics. It is assumed that the transfer process during heat treatment is a stationary diffusion process and the equilibrium state of reactions are held at a steel-inclusions interface, indicating that the concentration of substances at the interface are the equilibrium concentration. Therefore, Fick's first law, as shown Equation (7), can be used to describe the transformation.

$$J_{X,r} = -D_X \cdot A \cdot \frac{dc_X}{dr} = -D_X \cdot A \cdot \frac{c_X^b - c_X^*}{\delta} \tag{7}$$

where $J_{X,r}$ is the mass flux of X, kg/s; D_X is the diffusion coefficient of X, m^2/s; A is the area of the interface, m^2; c_X is the concentration of X, kg/m^3; r is the distance from the interface, m; δ is the boundary layer thickness, m. In this paper, superscript * represents the interface between the steel matrix and the inclusions, and b denotes the steel matrix.

$$J_{X,r} = \frac{dm_X}{dt} = V \cdot \frac{dc_X}{dt} \tag{8}$$

where m_X is the mass of X, kg; V is the volume of the inclusion or steel matrix, m^3; t is the diffusion time, s. Equation (7) is equal to Equations (8) and (9) can be obtained.

$$\frac{dc_X}{dt} = -\frac{D_X}{\delta} \cdot \frac{A}{V}\left(c_X^b - c_X^*\right) \tag{9}$$

Equation (10) derived from Equation (9) is usually utilized to describe the kinetic reaction of the steel matrix.

$$\frac{d[\%M]}{dt} = -\frac{n \cdot A_{steel-inc} \cdot k_{m\_inc}}{V_{steel}}\left([\%M]^b - [\%M]^*\right) \tag{10}$$

where $[\%M]$ is the mass percentage of M element; n is the number of inclusions; $A_{steel-inc}$ is the contact area between the steel matrix and inclusions, m^2; V_{steel} is the volume of the steel matrix, m^3; k_{m_inc}, defined as $\frac{D_M}{\delta}$, is the mass transfer coefficient of M element in the boundary layer, m/s.

However, the variation of the element content in the steel matrix, such as the dissolved oxygen, sulfur, and calcium cannot be measured during heat treatment due to the limitation of current detection methods. Besides, it is difficult to determine the contact area between the steel matrix and inclusions. The situation could be simplified when kinetic calculations were performed assuming that mass transfer takes place as the molecules of inclusion components between the steel matrix and inclusions, because the composition of inclusions can be obtained after heat treatment. Moreover, the inclusion diffusion was assumed as a rate-limiting step of reactions in current work. Consequently, Equation (11) can be applied to describe the kinetic reaction of inclusions. Equations (12) and (13) are derived from Equation (11).

$$\frac{d(\%MO_n)_{inc}}{dt} = -\frac{6 \cdot k_{inc}}{d_p}\left[(\%MO_n)^b_{inc} - (\%MO_n)^*_{inc}\right] \tag{11}$$

$$\ln\left[(\%MO_n)_{inc} - (\%MO_n)^*_{inc}\right] = -\frac{6k_{inc}}{d_p}t + C \tag{12}$$

$$\ln\left[(\%MO_n)^*_{inc} - (\%MO_n)_{inc}\right] = -\frac{6k_{inc}}{d_p}t + C \tag{13}$$

where $(\%MO_n)_{inc}$ is the mass percentage of MO_n in inclusions; k_{inc}, defined as $\frac{D_{MO_n}}{\delta}$, is the mass transfer coefficient of MO_n in the boundary layer, m/s; d_p is the diameter of the inclusions; C is the constant.

The mass percentage of MO_n in inclusions after a certain time of heat treatment and that at equilibrium state $(\%MO_n)^*_{inc}$ can be acquired from Figure 7, Figure 13, and Figure 14. As stated previously, the diameter of the inclusions d_p can be regarded as the constant value, according to Figure 16. Thus, k_{CaS} and k_{CaO} at different temperatures are obtained as empirical parameters shown in Figure 23. At 1498 K and 1573 K, the mass transfer coefficient of CaS in inclusions is larger than that of CaO, and they are almost the same at 1648 K. In addition, the mass transfer coefficient of CaS (or CaO) in inclusions at 1573 K is larger than that of CaS (or CaO) at 1498 and 1648 K.
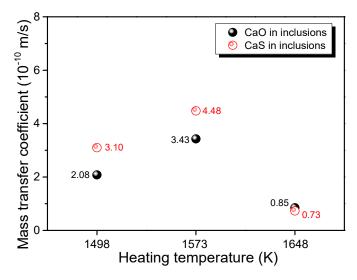

Figure 23. Effect of temperature on the mass transfer coefficient of inclusion components

Although Al_2O_3-CaO-(MgO) inclusions can transform to Al_2O_3-CaS-(MgO-CaO) during a high temperature diffusion process at 1498 K, it does not mean that inclusions in blooms should be controlled as calcium aluminate. The transformation of large calcium aluminate inclusions which are the most detrimental to bearing steels need longer time to complete, resulting in the increase of the production cost.

6. Conclusions

In the current study, laboratory experiments and thermodynamic and kinetic analyses were performed to investigate the transformation of inclusions in GCr15 bearing steels during heat treatment. The following conclusions were obtained:

1. Heat treatment of GCr15 bearing steels in the range of 1498 to 1648 K can transform Al_2O_3-CaO-(MgO) inclusions to Al_2O_3-CaS-(MgO-CaO) inclusions, mainly in the form of Al_2O_3-MgO enveloped by CaS. The reaction between Al and S in the steel matrix and CaO in the inclusions dominated the transformation at 1498 K, while the reaction between S in the steel matrix and CaO in the inclusions predominated at 1573 and 1648 K. The calculated and measured results are in good agreement.

2. The transformation rate of the inclusions depends strongly on both the temperature (in the range of 1498 K–1648 K) and the inclusion size. Small Al_2O_3-CaO-(MgO) inclusions transformed more severely than large ones. At the temperature for high temperature diffusion, 1498 K, the transformation reaction can reach an equilibrium state in 3 h, while at 1573 K, the time is only about 20 min. Although increasing the temperature from 1498 to 1573 K can accelerate the transformation of the inclusions, the effect of the temperature on the microstructure and segregation must be taken into consideration at the same time.

3. The mass transfer coefficients of CaO and CaS in inclusions are 2.08×10^{-10} m/s and 3.10×10^{-10} m/s at 1498 K, respectively. At 1573 K, the mass transfer coefficient of CaO is 3.43×10^{-10} m/s and that of CaS is 4.48×10^{-10} m/s. However, at 1648 K, the mass transfer coefficient of CaO is only 0.85×10^{-10} m/s and that of CaS is 0.73×10^{-10} m/s.

Author Contributions: Conceptualization, G.C. and W.L.; methodology, G.C. and W.L.; writing—original draft preparation, G.C.; writing—review and editing, L.Z. and X.Z.

References

1. Wang, S.; Qing, L.; Wang, H.; Mei, L. Behavior of non-metallic inclusions in casting slab of bof bearing steel. *J. Northeast. Univ. Nat. Sci.* **2006**, *27*, 192–195.
2. Monnot, J.; Heritier, B.; Cogne, J.Y. *ASTM STP 987 Relationship of Melting Practice, Inclusion Type and Size with Fatigue Resistance of Bearing Steels*; American Society for Testing Materials: West Conshohocken, PA, USA, 1988; p. 358.
3. Murakami, Y. Inclusion rating by statistics of extreme values and its application to fatigue strength prediction and quality control of materials. *Int. J. Fatigue* **1994**, *18*, 215. [CrossRef]
4. Hashimoto, K.; Fujimatsu, T.; Tsunekage, N.; Hiraoka, K.; Kida, K.; Santos, E.C. Study of rolling contact fatigue of bearing steels in relation to various oxide inclusions. *Mater. Des.* **2011**, *32*, 1605–1611. [CrossRef]
5. Hashimoto, K.; Hiraoka, K.; Kida, K.; Santos, E.C. Effect of sulphide inclusions on rolling contact fatigue life of bearing steels. *Mater. Sci. Technol.* **2012**, *28*, 39–43. [CrossRef]
6. Uesugi, T. Recent development of bearing steel in japan. *ISIJ Int.* **2006**, *28*, 893–899. [CrossRef]
7. Wang, Y.; Sridhar, S.; Valdez, M. Formation of CaS on Al_2O_3-CaO inclusions during solidification of steels. *Metall. Mater. Trans. B* **2002**, *33*, 625–632. [CrossRef]
8. Verma, N.; Pistorius, P.C.; Fruehan, R.J.; Potter, M.; Lind, M.; Story, S. Transient inclusion evolution during modification of alumina inclusions by calcium in liquid steel: Part I. Background, experimental techniques and analysis methods. *Metall. Mater. Trans. B* **2011**, *42*, 711–719. [CrossRef]

9.   Yang, S.; Wang, Q.; Zhang, L.; Li, J. Formation and modification of MgO·Al$_2$O$_3$-based inclusions in alloy steels. *Metall. Mater. Trans. B* **2012**, *43*, 731–750. [CrossRef]

10.   Verma, N.; Pistorius, P.C.; Fruehan, R.J.; Potter, M.S.; Oltmann, H.G.; Pretorius, E.B. Calcium modification of spinel inclusions in aluminum-killed steel: Reaction steps. *Metall. Mater. Trans. B* **2012**, *43*, 830–840. [CrossRef]

11.   Geldenhuis, J.M.A.; Pistorius, P.C. Minimisation of calcium additions to low carbon steel grades. *Ironmak. Steelmak.* **2013**, *27*, 442–449. [CrossRef]

12.   Ren, Y.; Zhang, L.; Li, S. Transient evolution of inclusions during calcium modification in linepipe steels. *ISIJ Int.* **2014**, *54*, 2772–2779. [CrossRef]

13.   Zhao, D.; Li, H.; Bao, C.; Yang, J. Inclusion evolution during modification of alumina inclusions by calcium in liquid steel and deformation during hot rolling process. *ISIJ Int.* **2015**, *55*, 2115–2124. [CrossRef]

14.   Yang, G.; Wang, X.; Huang, F.; Yang, D.; Wei, P.; Hao, X. Influence of calcium addition on inclusions in LCAK steel with ultralow sulfur content. *Metall. Mater. Trans. B* **2015**, *46*, 145–154. [CrossRef]

15.   Xu, G.; Jiang, Z.; Li, Y. Formation mechanism of CaS-bearing inclusions and the rolling deformation in al-killed, low-alloy steel with Ca treatment. *Metall. Mater. Trans. B* **2016**, *47*, 2411–2420. [CrossRef]

16.   Sun, K.K.; Kong, Y.M.; Park, J.H. Effect of Al deoxidation on the formation behavior of inclusions in Ce-added stainless steel melts. *Met. Mater. Int.* **2014**, *20*, 959–966.

17.   Wang, H.; Xiong, L.; Zhang, L.; Wang, Y.; Shu, Y.; Zhou, Y. Investigation of RE-O-S-As inclusions in high carbon steels. Metall. *Mater. Trans. B* **2017**, *48*, 1–10. [CrossRef]

18.   Reis, B.H.; Bielefeldt, W.V.; Vilela, A.C.F. Efficiency of inclusion absorption by slags during secondary refining of steel. *ISIJ Int.* **2014**, *54*, 1584–1591. [CrossRef]

19.   Hao, X.; Wang, X. A new sulfide capacity model for CaO-Al$_2$O$_3$-SiO$_2$-MgO slags based on corrected optical basicity. *Steel Res. Int.* **2016**, *87*, 359–363. [CrossRef]

20.   Chen, C.; Jiang, Z.; Li, Y.; Sun, M.; Qin, G.; Yao, C.; Wang, Q.; Li, H. Effect of Rb$_2$O on inclusion removal in C96V saw wire steels using low-basicity LF refining slag. *ISIJ Int.* **2018**, *58*, 2032–2041. [CrossRef]

21.   Shin, J.H.; Park, J.H. Effect of CaO/Al$_2$O$_3$ ratio of ladle slag on formation behavior of inclusions in Mn and V alloyed steel. *ISIJ Int.* **2018**, *58*, 88–97. [CrossRef]

22.   Zhang, L.; Liu, Y.; Zhang, Y.; Yang, W.; Chen, W. Transient evolution of nonmetallic inclusions during calcium treatment of molten steel. *Metall. Mater. Trans. B* **2018**, *49*, 1–19. [CrossRef]

23.   Pretorius, E.B.; Oltmann, H.G.; Cash, T. The Effective Modification of spinel inclusions by Ca-treatment in LCAK steel. *Iron Steel Technol.* **2010**, *7*, 31–44.

24.   Yang, G.; Wang, X.; Huang, F.; Wang, W.; Yin, Y.; Tang, C. Influence of reoxidation in tundish on inclusion for Ca-treated Al-killed steel. *Steel Res. Int.* **2014**, *85*, 784–792. [CrossRef]

25.   Wang, J.; Li, W.; Ren, Y.; Zhang, L. Thermodynamic and kinetic analysis for transformation of oxide inclusions in solid 304 stainless steels. *Steel Res. Int.* **2019**. [CrossRef]

26.   Ren, Y.; Zhang, L.; Pistorius, P.C. Transformation of oxide inclusions in type 304 stainless steels during heat treatment. *Metall. Mater. Trans. B* **2017**, *48*, 1–12. [CrossRef]

27.   Takahashi, I.; Sakae, T.; Yoshida, T. Changes of the nonmetallic inclusion by heating-study on the nonmetallic inclusion in 18-8 stainless steel (II). Trans. *Iron Steel Inst. Jpn.* **1967**, *53*, 350–352.

28.   Shibata, H.; Tanaka, T.; Kimura, K.; Kitamura, S.Y. Composition change in oxide inclusions of stainless steel by heat treatment. *Ironmak. Steelmak.* **2010**, *37*, 522–528. [CrossRef]

29.   Shibata, H.; Kimura, K.; Tanaka, T.; Kitamura, S.Y. Mechanism of change in chemical composition of oxide inclusions in Fe-Cr alloys deoxidized with Mn and Si by heat treatment at 1473 K. *ISIJ Int.* **2011**, *51*, 1944–1950. [CrossRef]

30.   Zou, X.; Zhao, D.; Sun, J.; Wang, C.; Matsuura, H. An integrated study on the evolution of inclusions in EH36 shipbuilding steel with Mg addition: From casting to welding. *Metall. Mater. Trans. B* **2017**, *49*, 1–9. [CrossRef]

31.   Wang, Q.; Zou, X.; Matsuura, H.; Wang, C. Evolution of inclusions during the 1473 K (1200 °C) heating process of EH36 shipbuilding steel. *Metall. Mater. Trans. B* **2018**, *49*, 18–22. [CrossRef]

32.   Chu, Y.; Li, W.; Ren, Y.; Zhang, L. Transformation of inclusions in linepipe steels during heat treatment. *Metall. Mater. Trans. B* **2019**. [CrossRef]

33.   Yang, W.; Guo, C.; Li, C.; Zhang, L. Transformation of inclusions in pipeline steels during solidification and cooling. *Metall. Mater. Trans. B* **2017**, *48*, 2267–2273. [CrossRef]

34. Liu, J.; Han, J.; Xi, J.; Zhao, J. Study of temperature and carbide solution diffusion for GCr15 bearing steel. *Heat Treat. Met.* **2008**, *133*, 87–90.

35. Holappa, L.; Hamalainen, M.; Liukkonen, M.; Lind, M. Thermodynamic examination of inclusion modification and precipitation from calcium treatment to solidified steel. *Ironmak. Steelmak.* **2002**, *30*, 111–115. [CrossRef]

36. Park, J.H.; Todoroki, H. Control of MgO·Al$_2$O$_3$ spinel inclusions in stainless steels. *ISIJ Int.* **2010**, *50*, 1333–1346. [CrossRef]

37. Lu, D.; Irons, A.; Lu, W. Kinetics and mechanisms of calcium dissolution and modification of oxide and sulphide inclusions in steel. *Ironmak. Steelmak.* **1994**, *21*, 362–371.

38. Harada, A.; Maruoka, N.; Shibata, H.; Kitamura, S.Y. A kinetic model to predict the compositions of metal, slag and inclusions during ladle refining: Part 1. Basic concept and application. *ISIJ Int.* **2013**, *53*, 2110–2117. [CrossRef]

39. Harada, A.; Maruoka, N.; Shibata, H.; Kitamura, S.Y. A kinetic model to predict the compositions of metal, slag and inclusions during ladle refining: Part 2. Condition to control the inclusion composition. *ISIJ Int.* **2013**, *53*, 2118–2125. [CrossRef]

40. Scheller, P.R.; Shu, Q. Inclusion development in steel during ladle metallurgical treatment—A process simulation model-part: Industrial validation. *Steel Res. Int.* **2014**, *85*, 1310–1316. [CrossRef]

41. Liu, Z.; Gu, K.; Cai, K. Mathematical model of sulfide precipitation on oxides during solidification of Fe-Si alloy. *ISIJ Int.* **2002**, *42*, 950–957. [CrossRef]

42. Fukumoto, S.; Iwasaki, Y.; Hikasa, Y. Selection of sulfide morphology in SUS303 during solidification. *ISIJ Int.* **2016**, *56*, 1023–1030. [CrossRef]

43. Kim, W.Y.; Kang, J.G.; Park, C.H.; Lee, J.B.; Pak, J.J. Thermodynamics of aluminum, nitrogen and AlN formation in liquid iron. *ISIJ Int.* **2007**, *47*, 945–954. [CrossRef]

44. Choi, W.; Matsuura, H.; Tsukihashi, F. Effect of nitrogen on the formation and evolution of non-metallic inclusions in Fe–Al–Ti–N alloy. *ISIJ Int.* **2013**, *53*, 2007–2012. [CrossRef]